LAST COPY

The Global Atmosphere and Ocean System, 1998, Vol. 6, pp. 243–268

Reprints available directly from the publisher
Photocopying permitted by license only

VALIDATION OF NCEP'S OCEAN WINDS FOR THE USE IN WIND WAVE MODELS*

HENDRIK L. TOLMAN**

Ocean Modeling Branch, Environmental Modeling Center, NOAA/NCEP, 5200 Auth Road, Room 209, Camp Springs, MD 20746

(Received 20 February 1997; In final form 6 March 1998)

The quality of analyzed ocean surface winds from the Global Data Assimilation System (GDAS) and forecasted winds from the early or 'aviation' cycle of the global medium range forecast model (AVN) of the National Centers for Environmental Prediction (NCEP) is assessed as part of a validation study of a new wave forecast system. This validation is performed using conventional buoy data and satellite retrieved wind speeds from the ERS1 altimeter and scatterometer. Both GDAS and AVN wind fields are shown to include moderate systematic biases, for which statistical corrections based on both satellite and buoy data are presented. Furthermore, buoy data are shown not to be representative for a global validation study.

The altimeter data are potentially of significant importance for wave model validations, as they include collocated wind and wave measurements. The altimeter winds, however, are shown to be seriously contaminated by the development stage of the wave field. As it does not appear to be possible to remove this contamination, altimeter wind data should not be used in the validation of wave models.

Keywords: NCEP winds; wave model; altimeter wind/waves

1. INTRODUCTION

This paper presents the first part of a validation study of a new ocean wind-wave forecast system at the National Centers for Environmental Prediction (NCEP). Wave forecast systems consist of two parts; a model for near-surface winds, and a model to predict waves based on these winds. The new NCEP forecast system takes its wind from NCEP's operational Global Data Assimilation System (GDAS, Derber *et al.*, 1991; Parish and Derber, 1992)

* OMB contribution Nr. 150.
** UCAR visiting scientist.

and from the early or 'aviation' cycle of the operational medium range forecast system (generally denoted as AVN, Kanamitsu 1989; Kanamitsu *et al.*, 1991). The wave model is a recent version of WAVEWATCH (Tolman, 1991). This paper presents the validation and statistical correction of the wind fields. Subsequent papers will present a validation of the wave model and of the entire forecast system.

Wave heights approximately scale with the square of the wind speed. This implies that an error of 10% in the wind speed leads to an error of 20% in the wave height. Wave forecast errors therefore are often dominated by errors in the wind fields, and it is thus important for both the forecast system and for an intercomparison of wave models to obtain the best possible wind fields. Here, the GDAS and AVN wind fields are validated and where possible corrected using buoy observations and remotely sensed wind speeds from satellites. These data cover a three month period from Dec. 1994 through Feb. 1995.

Wind fields are generally validated with *in situ* measurements from buoys. Unfortunately, buoy data do not provide global coverage (Fig. 1), and hence the corresponding validation cannot claim global validity. Global validation can only be obtained with satellite data. Of particular interest for the present study are altimeter data, as they provide collocated wind and wave estimates. Such collocated data can potentially be used to separate wind input errors from wave model errors in a wave forecast system. However, satellite-retrieved winds are generally inferred rather than direct

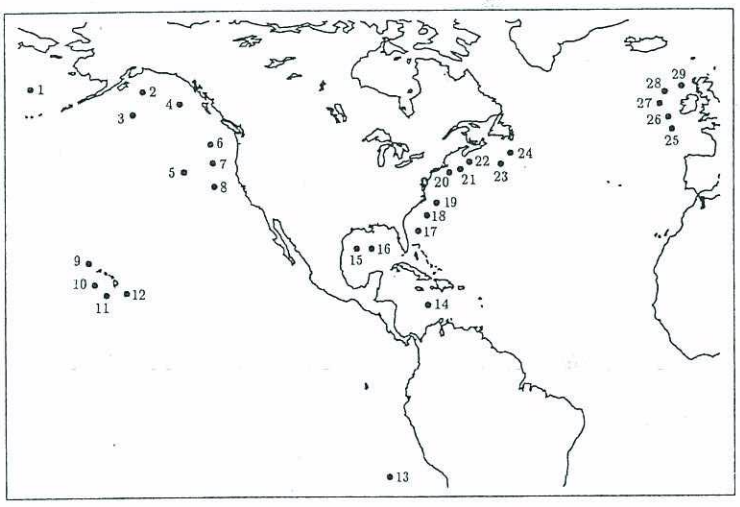

FIGURE 1 Buoy locations. Numbering as in Table I.

measurements. Because the algorithms are tuned or validated with buoy data, their global validity is also in question. This is particularly true for the altimeter wind speeds, as they are potentially contaminated by swell. the present study therefore also includes scatterometer data from ERS1.

The wind driving the wave model is inherently a vector quantity. The present study, however, concentrates on the scalar wind speed for several reasons. (i) Potential impact: wind speed correction has a potentially large impact on a wave model due to the roughly quadratic scaling behavior. Wind directions are more or less uniformly distributed over its entire domain, and are therefore expected to incorporate random rather than systematic errors. (ii) Data availability: the altimeter does not provide an estimate of the wind direction, whereas the scatterometer wind directions require (subjective) ambiguity removal (up to four solutions). This makes it difficult or even impossible to consider the full wind vector A consistent analysis considers the same parameter for all instruments, *i.e.*, the wind speed. (iii) Ease of correction: wind speeds are easily corrected. For the GDAS winds, the underlying assumption of such a correction could be that the weather patterns are generally well analyzed, but that the corresponding wind speeds have systematic biases. This is consistent with the experience of NCEP's operational forecasters (personal communication). Vector wind corrections are much more complicated. The additional complication is not justified by the expected small impact of correcting wind directions. Note that scalar wind speeds from GDAS and AVN at buoy locations and satellite tracks are obtained by vector interpolation unless specified differently.

The layout of this paper is as follows. In Section 2 the wind fields and data are discussed. In Section 3 analysis techniques are described briefly.

In Section 4, the GDAS and AVN wind fields are validated against the buoy data. In Section 5 the GDAS and AVN wind fields are validated with satellite data. The latter validation includes bias corrections and an assessment of global validity of altimeter and scatterometer winds. In the final discussion in Section 6 systematic and random errors of the GDAS and AVN winds are separated, and statistical corrections for systematic errors are suggested. Furthermore, the quality of altimeter wind speeds is considered for the use in subsequent parts of this study.

2. WINDS

As described in the introduction, the wind fields of the wave forecast system are obtained from NCEP's GDAS and AVN. The 48 h forecast will be

considered representative for the forecast winds for the wave model and will simply be denoted as the AVN winds. The spectral resolution of the wind fields is T126. For the use in the wave forecast, the lowest level winds are extracted on $1.25° \times 1°$ longitude-latitude grid. The winds are converted from their nominal height of 35 m to 10 m assuming neutral atmospheric stratification. The time interval between wind fields if 6 h. In the wave model, the wind speed and direction are separately interpolated in time to hourly values. Compared to wind fields which are kept constant for 6 h intervals, this reduces the standard deviation relative to hourly buoy observations by approximately 20%, with a minor impact on biases (figures not presented).

Hourly data for the 29 buoys presented in Figure 1 and Table I have been obtained from the operational archive at NCEP. One of these buoys reported wave data only, and is therefore not used in the present part of the

TABLE I Buoys used in the wave forecast system validation study

	WMO ID number	*Location*		*Anemometer height (m)*	*Region*
1	46035	57.0°N	177.7°W	10.0	
2	46003	51.9°N	150.9°W	5.0	
3	46001	56.3°N	148.3°W	5.0	
4	46184	53.9°N	138.8°W	5.0	A
5	46006	40.8°N	137.8°W	5.0	
6	46005	46.1°N	131.0°W	5.0	
7	46002	42.5°N	130.4°W	5.0	
8	46059	38.0°N	130.0°W	5.0	
9	51001	23.4°N	162.3°W	5.0	
10	51003	19.2°N	160.8°W	5.0	B
11	51002	17.2°N	157.8°W	5.0	
12	51004	17.5°N	152.6°W	5.0	
13	32302	18.0°S	85.1°W	5.0	
14	41018	15.0°N	75.0°W	5.0	C
15	42002	25.9°N	93.6°W	10.0	
16	42001	25.9°N	89.7°W	10.0	
17	41006	29.3°N	77.4°W	5.0	
18	41002	32.3°N	75.2°W	5.0	
19	41001	34.7°N	72.7°W	5.0	
20	44008	40.5°N	69.4°W	5.0	D
21	44011	41.1°N	66.6°W	5.0	
22	(44142)	42.5°N	64.2°W	5.0	
23	44141	42.1°N	56.1°W	5.0	
24	44138	44.2°N	53.6°W	5.0	
25	62029	48.7°N	12.4°W	4.0	
26	62081	51.0°N	13.3°W	4.0	
27	62108	53.6°N	15.5°W	4.0	E
28	62105	55.9°N	14.2°W	4.0	
29	62106	57.0°N	9.9°W	4.0	

validation study. NCEP obtains this data from near real-time GOES and GTS transmissions. All wind speeds have been converted to a common height of 10 m, using the anemometer height as presented in Table I and assuming neutral stratification. This data set consists of over 42,000 observations.

Two types of ERS1 products are available; the 'fast delivery' products, which are distributed in near real time, and the 'operational' products, which are distributed with some delay. Because the ERS1 data are also used in operational models, NCEP and the present study exclusively use fast delivery data. The fast delivery data might be expected to be of somewhat lesser quality than the operational data. This is not expected to be a problem, because both systematic and random wind speed errors are explicitly estimated and accounted for in the present study (Sections 5 and 3).

ERS1 fast delivery altimeter data include (amongst others) a direct measurement of the wave height, and an estimate of the wind speed based on the algorithm of Witter and Chelton (1991). The wind speed is inferred from high-frequency wave energy, and is potentially sensitive to the development stage of the wave field and the presence of background swells (*e.g.*, Brown, 1979; Glazman and Pilorz, 1990; Lefevre *et al.*, 1994). Furthermore, the algorithm saturates at high wind speeds, with a maximum retrievable wind speed of approximately 21 ms^{-1}(Witter and Chelton, 1991). These wind and wave data are regularly used at NCEP for validation of, and data assimilation into the operational global wave model. For this purpose, the original data are averaged along the satellite track for 10 s intervals (corresponding to a 65 km data separation) and quality controlled. These averaged data are used in the present study (3.1×10^5 obs.), and will be denoted as the ALT data.

Additional wind speed estimates are obtained from the ERS1 scatterometer. These data are archived routinely at NCEP at their native resolution, and are obtained through the National Environmental Satellite Data Information Service (NESDIS). The fast delivery wind speeds (see Ofiller, 1994) are used without further averaging. These data will be denoted as the SCAT data (8.9×10^6 obs.). Like the ALT wind speeds, the SCAT wind speeds are inferred from high-frequency wave energy, and therefore have a similar potential dependency on the stage of development of the wave field. Due to a different look angle, the SCAT data are expected to be less sensitive to swell than the ALT data. The SCAT wind speed is expected to saturate at high wind speeds, but the saturation level is not well documented.

3. ANALYSIS TECHNIQUES

Winds speed errors will be assessed in this study using (amongst others) linear regression techniques and the analysis of model results for narrow bins of observed wind speeds (bin-averaged or BA analyses). The first type of analysis provides a simple and robust way to assess overall model behavior. The latter analysis is more detailed, and is mostly used to assess nonlinear model behavior and model behavior for high wind speeds.

In a linear regression analysis, the model wind speed u_m is approximated as a linear function of the observed wind speed u_o

$$u_m = a + bu_o, \tag{1}$$

where b is the regression coefficient and a is the intercept. Regression lines obtained with different techniques generally have the point $(\overline{u_m}, \overline{u_o})$ in common, where the overbar denotes the average of all observations. In a conventional regression analysis, the rms difference between (1) and the model wind speed u_m is minimized. If the observations are free of errors, this technique gives an accurate estimate of the model behavior, and (1) can be used to estimate the model bias. In most studies, however, the observation includes a noticeable random error due to instrument errors, data truncation, collocation, scale differences between model and observations, *etc.* In such conditions, a conventional regression analysis systematically underestimates the regression coefficient b (*e.g.*, Lindley, 1947; Ricker, 1973; Draper and Smith, 1981; Section 2.14), which in turn introduces systematic analysis errors if (1) is used to estimate the model bias. If the observation error can be estimated, such analysis errors can be largely corrected (Tolman, 1998). The corresponding regression coefficient is estimated as

$$b = \frac{s_{om}}{s_{oo} - \overline{\sigma_o^2}}, \tag{2}$$

where $s_{oo} = \overline{u_o^2} - \overline{u_o}^2$ is the variance of the observations, $s_{om} = \overline{u_o u_m} - \overline{u_o}\,\overline{u_m}$ is the covariance of the data, and $\overline{\sigma_o}$ is a standard deviation of the random observation error, representative for the entire data set.

In a BA analysis the mean model wind speed $\overline{u_m}(u_o)$ and the random model error $\sigma_m(u_o)$ are determined for a number of small wind speed intervals ('bins') δu_o. The finite bine size δu_o induces an overestimation of the random model error, and a random observation error $\sigma_o(u_o)$ induces (i) a systematic underestimation of extreme wind speeds, (ii) spurious nonlinearity in the analysis, and (iii) an overestimation of the random model error

(Tolman, 1998). If $\sigma_o(u_o)$ can be estimated, the errors of a BA analysis can be estimated by (iteratively) convoluting the data with the observation error. The error-corrected BA analysis is implemented here as described in Section 4 of Tolman (1998).

Below, the error-corrected regression (2) and BA analysis will be denoted simply as regression and BA analyses.

4. VALIDATION WITH BUOY DATA

First, the GDAS and AVN wind fields will be validated with buoy data. The above analysis techniques require an estimate of the random observation error. This estimate is discussed in the appendix.

Figure 2 shows results of the validation of the GDAS winds with all buoy data. In the BA analysis a bin width of $1\,\mathrm{ms}^{-1}$ and a minimum number of observations of 20 and 40 have been used for the bias $\beta = u_m - u_o$ and the random error, σ, respectively. The GDAS moderately overestimates small wind speeds (∘ in panel a, $u < 10\,\mathrm{ms}^{-1}$), and underestimates higher wind speeds. This bias is a nearly linear function of the observed wind speed u, and closely follows the regression line (compare ∘ and dashed line in panel a). Although the uncertainty in the BA analysis due to the uncertainty in the estimate of the observation error is appreciable (shaded area), it does not influence results qualitatively. The GDAS wind fields indeed incorporate less extreme wind speeds than the corresponding buoy data, as is illustrated in Table II. The estimated random error (∘ in panel b) is approximately $1.3\,\mathrm{ms}^{-1}$, for wind speeds up to $15\,\mathrm{ms}^{-1}$, and increases somewhat for higher wind speeds. Note that good validation statistics against buoy data might be expected, as some of the buoy data are used in the GDAS analysis.

Figure 3 shows the corresponding results for the AVN winds. As expected, biases (β) and random errors (σ) are larger than for the GDAS, but are qualitatively similar for the bulk of the data ($5 < u < 15\,\mathrm{ms}^{-1}$). For wind speeds over $20\,\mathrm{ms}^{-1}$, which represent only 0.7% of all data, the AVN shows a strongly nonlinear negative bias (∘ in Fig. 3a). In contrast, the extreme wind speed distribution of the AVN follows observations even better than the GDAS (Tab. II). Thus, the strongly negative bias for $u > 20\,\mathrm{ms}^{-1}$ does not identify a systematic underestimation of extreme events, but has to be attributed to random errors in the location and strength of such events.

The large number of buoy data makes it possible to assess the quality of the winds fields for separate regions. Regions considered are (A) the Gulf of

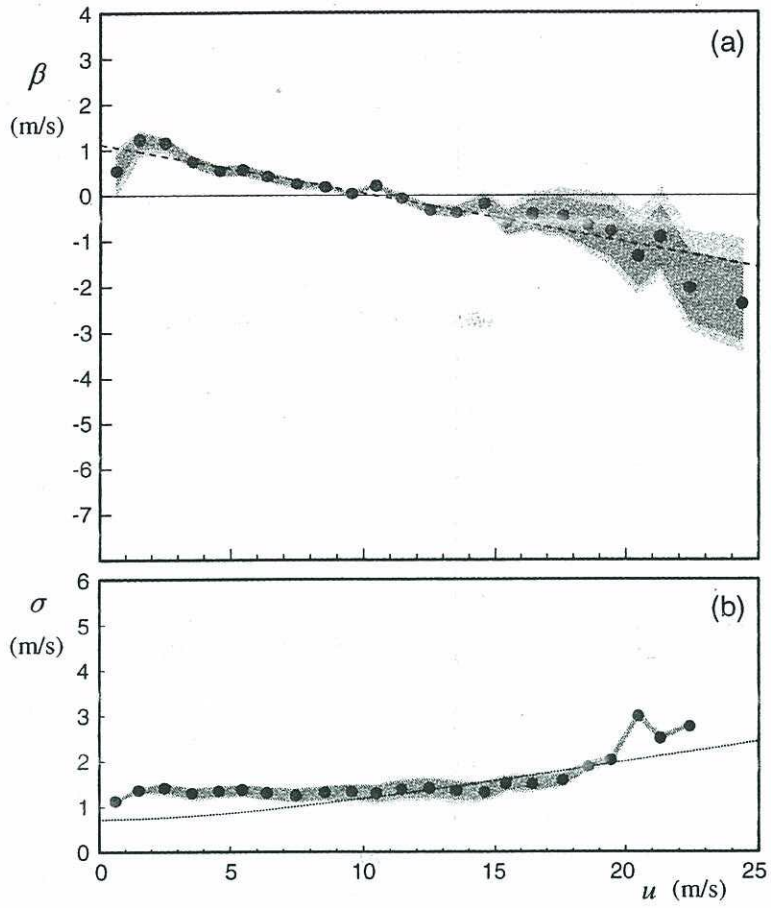

FIGURE 2 Bias β (panel a) and standard deviation of random error σ (panel b) as a function of the observed wind speed u for the GDAS winds relative to buoy observations. •: BA analysis with 1 m/s bin width and a minimum of 20 observations for β and 40 observations for σ. $\alpha = 0.7$ and $\gamma_0 = 0.13$ in Eqs. (A2) and (A3). Light shading: results for $0.6 < \alpha < 0.8$ and γ_0 varying as in Table A1. Dark shading: variation of γ_0 only. Dashed line: linear regression.

TABLE II Distribution of extreme wind speeds in the collocation of GDAS and AVN winds with buoy data. Total number of data 42,171. 'cor.' denotes GDAS wind speeds corrected according to Eq. (4)

$u >$	*Number of occurrences*			
(ms^{-1})	*Buoy*	*GDAS*	*Cor.*	*AVN*
20.0	321	153	284	329
22.5	86	33	70	72
25.0	29	9	18	15
27.5	8	1	6	2
30.0	2	0	1	1

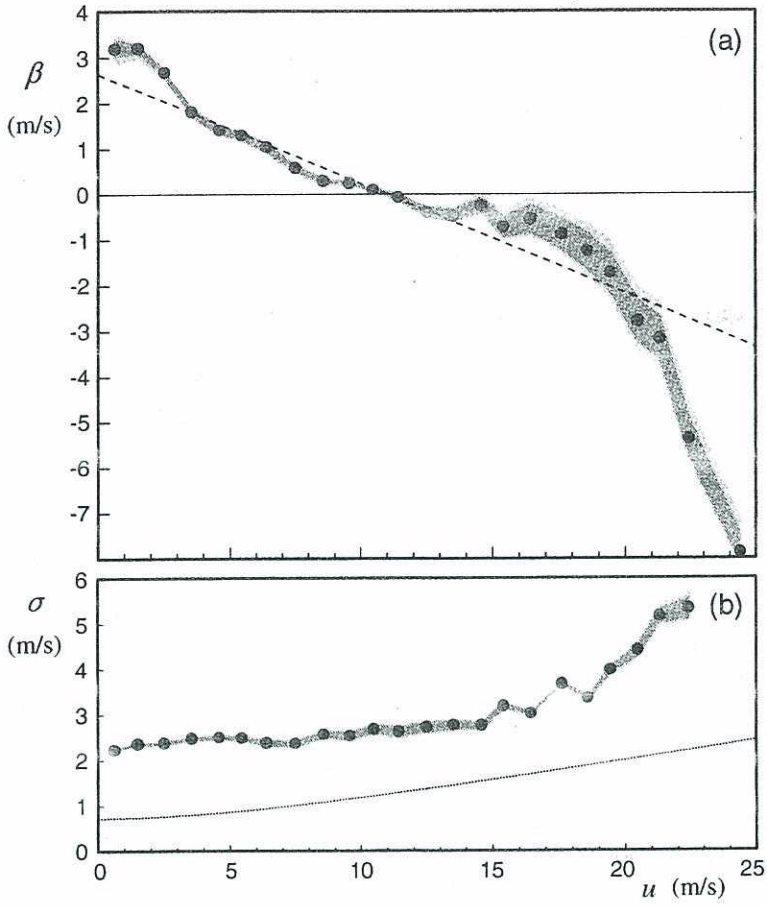

FIGURE 3 Like Figure 2 for the AVN winds.

Alaska, (B) Hawaii, (C) the 'tropics', (D) the east coast of the North America, and (E) the British Isles (see Tab. I). Biases β per region are presented in Figure 4. To highlight systematic behavior, the biases are represented by third-order polynomial fits to the BA results.

Figure 4a shows biases in each region for the GDAS winds. The separate regions (dashed lines) show a random behavior relative to the composite data set (solid line). The biases are practically linear functions of the observed wind speed for all regions. Figure 4b shows biases in each region for the AVN. All regions show a similar nonlinear increase of a positive bias for low wind speeds (dashed lines). Regions A and E are solely responsible for the nonlinear negative biases at high wind speeds in Figure 3. These

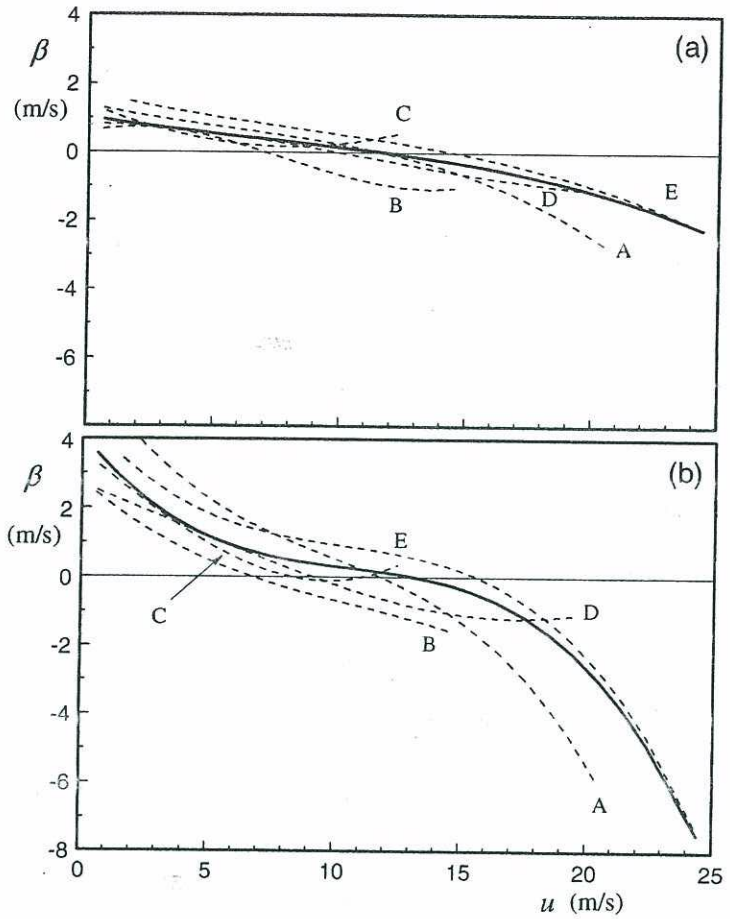

FIGURE 4 Biases β per region relative to buoy observations. Regions as in Figure 1 and Table I. Third-order polynomials fit to BA results. Solid line represents all data. (a) GDAS. (b) AVN.

regions are downstream of data–sparse areas, so that larger random forecast errors might be expected. In contrast, high wind speeds in area D are well predicted. This area is downstream of a data-rich area. Apparently, random forecast errors are much smaller here.

5. VALIDATION WITH SATELLITE DATA

Unfortunately, the buoy data used in the previous section cover only selected regions. A global assessment of the quality of the wind fields can

only be obtained from satellite data. Before such satellite data are used, their quality should be assessed; biases should be removed and estimates of random errors are required for the regression and BA analyses. Note that such a bias correction automatically accounts for incompatibilities representative observation heights.

a. Quality of Data

To assess the quality of satellite wind speed retrievals, they have been collocated with buoy data. The collocation radii as presented in Table III are mostly dictated by the need for a reasonable number of collocations. In particular for the altimeter, the fairly large radius R might result in a significant random collocation error. Note that this random error is explicitly estimated and accounted for in the new statistical techniques used here (see Section 3 and Tolman, 1998).

Buoy observation errors with respect to the satellite data are discussed in the appendix. Biases β and random errors σ for the satellite based wind speeds are presented in Figures 5 and 6. Both satellite derived wind speeds show significant biases. Unfortunately, the number of collocated data are relatively small. This results in a significant sampling variability, and a limited range of wind speeds for which errors are estimated. Both drawbacks do not justify a detailed bias removal. Therefore, simple linear corrections as presented in Table IV are applied to each data set. To retain a maximum consistency for mean biases, the corrections correspond to the regression lines. To eliminate the possibility of linear corrections resulting in negative wind speeds, they are replaced by a quadratic form for low wind speeds, with no correction for $u = 0$ and constant functional and first derivative at the connection point. The transition occurs for $u = 2.5\,\mathrm{ms}^{-1}$.

The ALT data show significantly larger random errors σ than the SCAT data (compare Figs. 5b and 6b), particularly for lower wind speeds. This might well be due to the potentially larger sensitivity of the ALT data to the presence of swell. To investigate such dependencies, the collocated ALT and

TABLE III Satellite-buoy collocation information. Collocations within a 30 min time frame, making average time separation 15 min. Only the closest collocation per satellite pass is considered. $R(r)$ is maximum (average) collocation distance

Data	*R* (*km*)	*r* (*km*)	*Number of col.*
ALT	100	48	270
SCAT	50	16	454

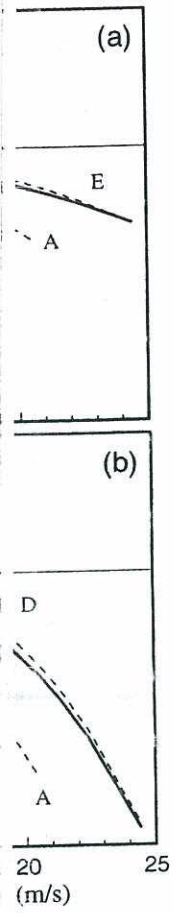

gions as in Figure 1 and
ts all data. (a) GDAS. (b)

that larger random
nd speeds in area D
ch area. Apparently,

section cover only
f the wind fields can

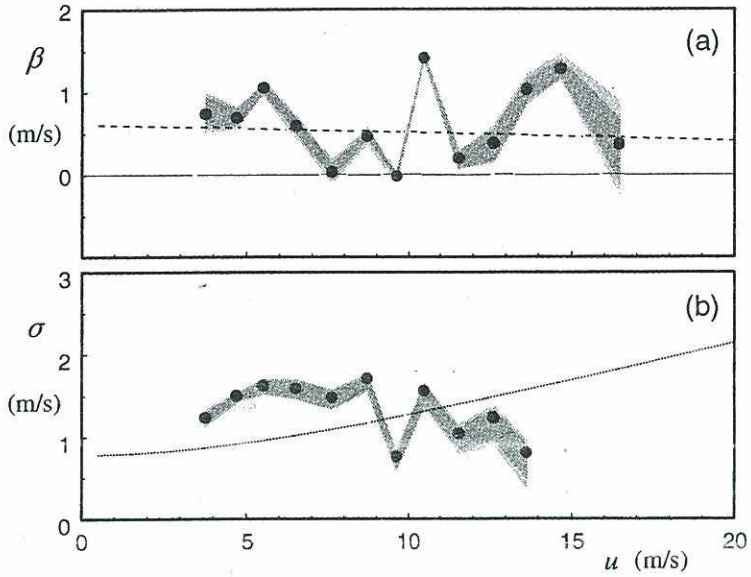

FIGURE 5 Like Figure 2 for ALT instrument errors. Minimum number of data for β and σ are 5 and 10, respectively.

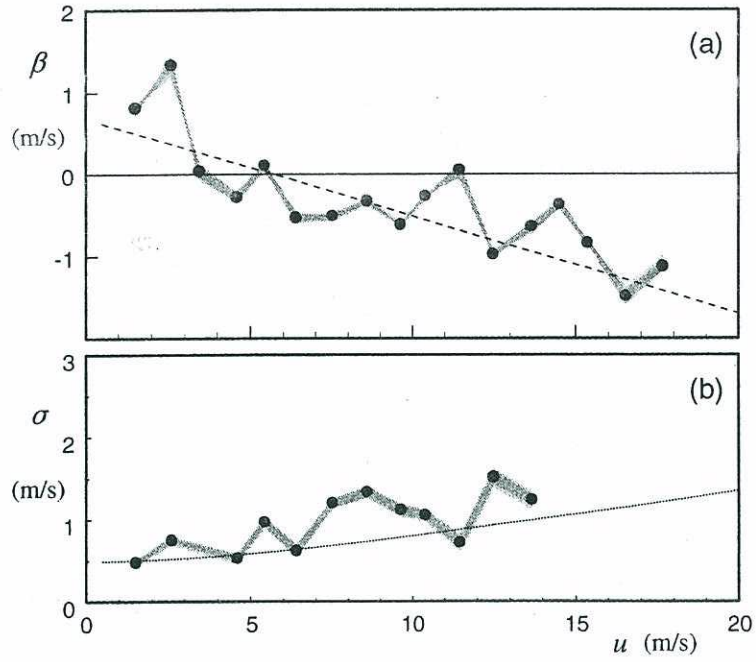

FIGURE 6 Like Figure 2 for SCAT instrument errors. Minimum number of data for β and σ are 7 and 14, respectively.

TABLE IV Satellite bias correction and observation errors relative to GDAS and AVN wind fields

Data	*Corrected speed*	*Observation error*
ALT	$-0.61\,\mathrm{ms}^{-1} + 1.01\,u$	$\max(1.35\,\mathrm{ms}^{-1}, 0.1\,u_o)$
SCAT	$-0.76\,\mathrm{ms}^{-1} + 1.14\,u$	$\max(0.90\,\mathrm{ms}^{-1}, 0.1\,u_o)$

SCAT data are stratified with the nondimensional wave height $\tilde{H}$

$$\tilde{H} = 3.33gHu^{-2}, \tag{3}$$

where H is the wave height. $\tilde{H} \approx 1$ for fully developed seas, $\tilde{H} < 1$ for developing wind seas, and $\tilde{H} > 1$ for overdeveloped wind seas and swells. Results of this data stratification are presented in Figure 7. The ALT data (Fig. 7a) show a distinct dependency of the regression lines on the selected range of $\tilde{H}$, indicating that the ALT data are indeed sensitive to the presence of swell. Because swell climates vary regionally, this suggests that the ALT data might include significant regional biases. The SCAT data, however, do not show a distinct dependency on $\tilde{H}$, and are therefore expected to have a consistent global validity.

b. Validation

As the satellite data are mainly of interest for their global coverage, global mean biases will be assessed first. Such biases are obtained by collocating GDAS and satellite data on a global $1° \times 1.25°$ latitude-longitude grid for the entire three month period considered here (Fig. 8). The ALT data and to a lesser extend the SCAT data are provided in narrow tracks. The consistency of the data is therefore much larger in latitudinal direction (along the tracks), than in longitudinal direction (across the track), and clear signatures of tracks can be found in the resulting average wind speeds and biases. To reduce longitudinal noise related to track signatures, some longitudinal smoothing has been applied to the average wind speeds and biases, with a filter width of approximately 7° and 5°, for ALT and SCAT collocations, respectively. Comparisons of the AVN wind speeds with the satellite retrievals proved similar, and are therefore not presented here.

Figure 8a shows the mean GDAS wind speeds for the collocations with the ALT data. The highest wind speeds occur at high latitudes in the northern hemisphere, corresponding to winter storms. Higher wind speeds furthermore occur in the ITCZ (0–15°N), and at high latitudes in the southern hemisphere. Mean GDAS wind speeds from collocation with

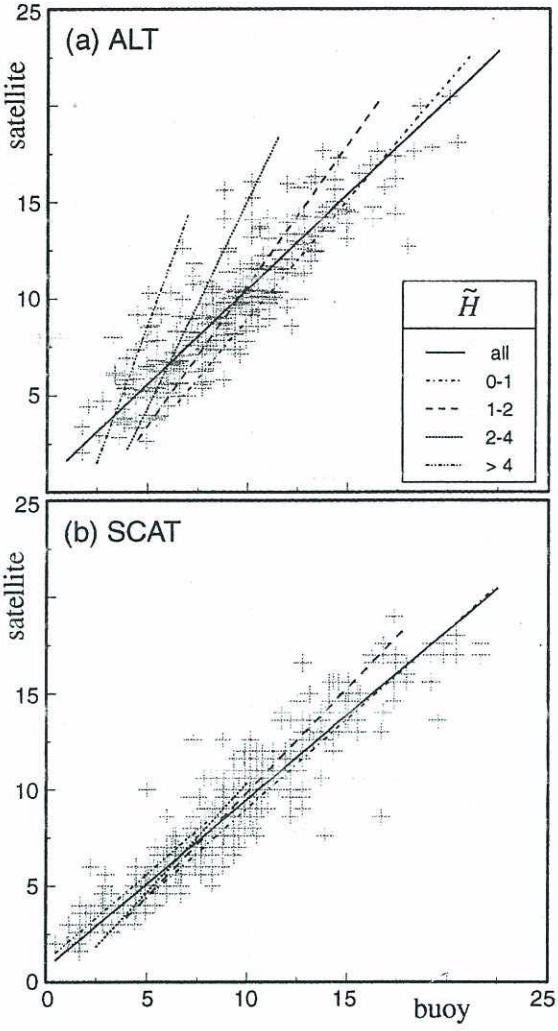

FIGURE 7 Collocated satellite and buoy wind speeds (in ms^{-1}) stratified with the nondimensional wave height $\tilde{H}$ (3). (a) ALT. (b) SCAT. Lines: linear regression for given range of $\tilde{H}$. + data. $\tilde{H}$ calculated from buoy data.

SCAT data show a similar distribution, suggesting that the collocations sample the synoptic wind fields in a similar way (figures not presented here). Figures 8b and 8c show GDAS mean biases as estimated from the two satellite data sets. Both satellite data sets suggest that the GDAS wind speeds incorporate a moderate but systematic positive bias. In particular for the scatterometer the buoys appear to be in areas with small biases, and in

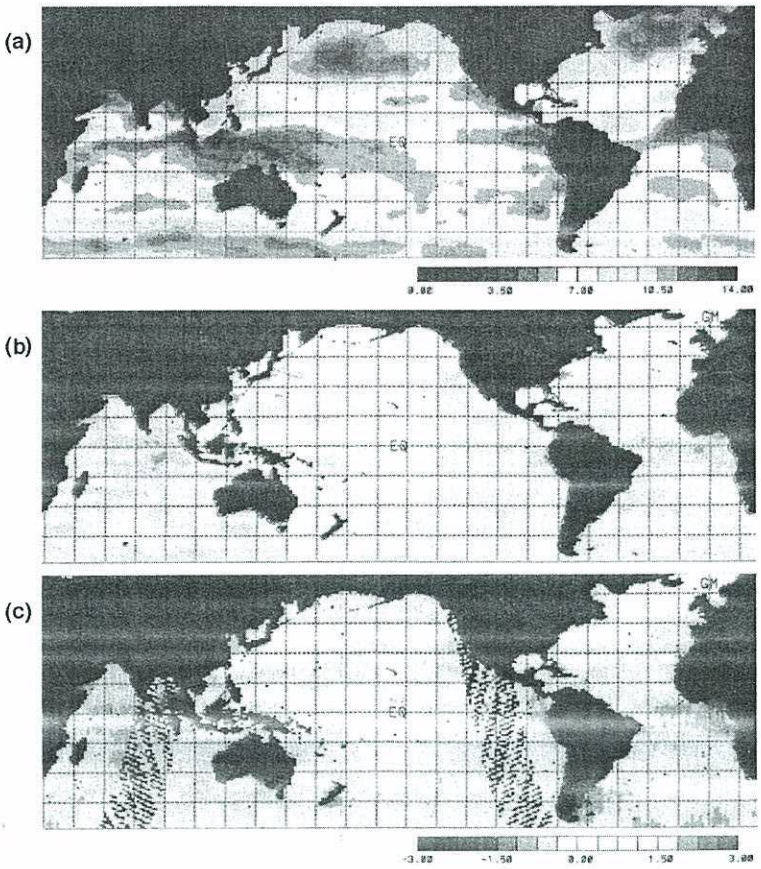

FIGURE 8 Collocated GDAS and satellite wind speeds on a 1° × 1.25° latitude–longitude grid. (a) mean GDAS wind speed for ALT collocations (ms^{-1}, legend under panel a). (b) GDAS bias relative to SCAT data (GDAS-SCAT in ms^{-1}, minimum of 50 observations per grid box, legend under panel c). (c) Idem, ALT data (7 observations or more). Black grid boxes denote insufficient data. Grid lines at 15° intervals. Satellite data bias–corrected as in Table IV. (See Color Plate I).

rare areas where the GDAS wind speeds appear to be biased low (*i.e.*, the east coast of the USA, Figs. 1 and 8b). A validation with buoy data can therefore not be completely representative for the global wind fields.

Figure 9 shows biases and random errors as a function of the observed wind speed for four latitude bands. These results are less reliable than the corresponding biases estimated from the buoy data because of uncertainties in the bias corrections of the satellite data, and because of the generally suspect nature of satellite retrievals of extreme wind speeds. For instance,

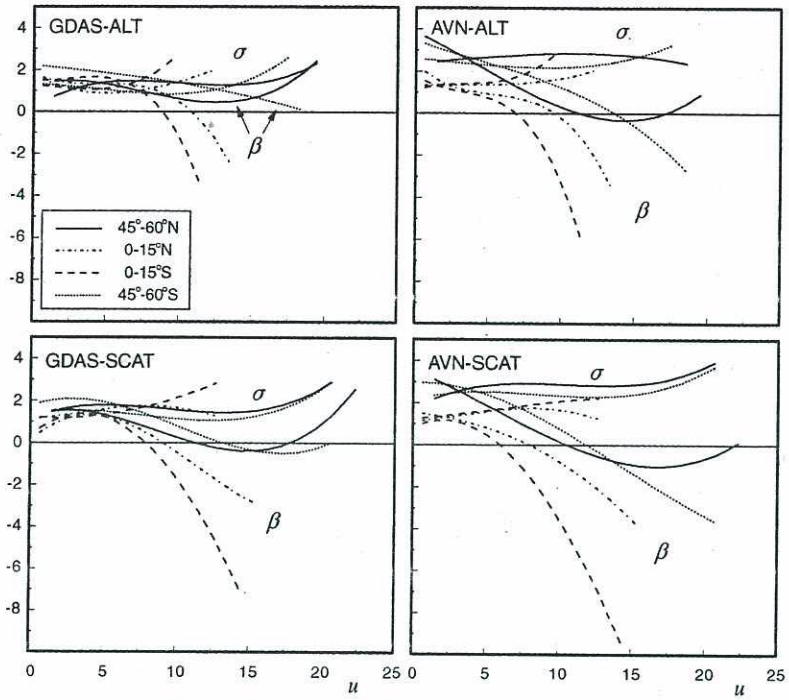

FIGURE 9 GDAS and AVN biases β and random errors (in ms^{-1}) as a function of the observed wind speed u as estimated from ALT and SCAT data for four latitude bands. Biases and random errors represented by third-order polynomials. Note that σ is definite positive, whereas β has negative values in all except two lines in the upper left panel.

the reduced negative bias for the highest wind speeds at northern high latitudes (solid lines for β in all panels), is an artifact of the saturation of the corresponding algorithms for high wind speeds. Again, several details of the results stand out: (i) Biases β are somewhat larger than biases estimated from the buoy observations, and (ii) Show a stronger dependency on the wind speed, particularly in the tropics. (iii) Biases increase mildly during the forecast. (iv) Random errors σ are fairly similar for all latitudes in GDAS. (v) In the AVN, random errors grow significantly at high latitudes, but remain relatively unchanged in the tropics.

The dependence of the biases on the wind speeds can be caused by both systematic and random forecast errors (as discussed for Fig. 3). Due to the suspect nature of satellite retrievals at high wind speeds, systematic and random errors cannot be separated by intercomparing distributions of extreme wind speeds. Alternatively, systematic errors can be isolated by determining mean biases as a function of mean wind speeds for selected

regions. In such mean parameters random errors cancel, the satellite bias correction becomes statistically more stable, and effects of retrieval errors for extreme wind speeds become small, as extreme wind speeds represent a minor fraction of the data. Because (average) wind conditions mostly vary with latitude, averaging over latitude bands will be performed. Mean biases for nine latitude ranges are presented in Figure 10. The right most symbols correspond to the high mean wind speeds in the most northerly latitude band (60–75°N). Following the dotted lines, results for consecutive latitude

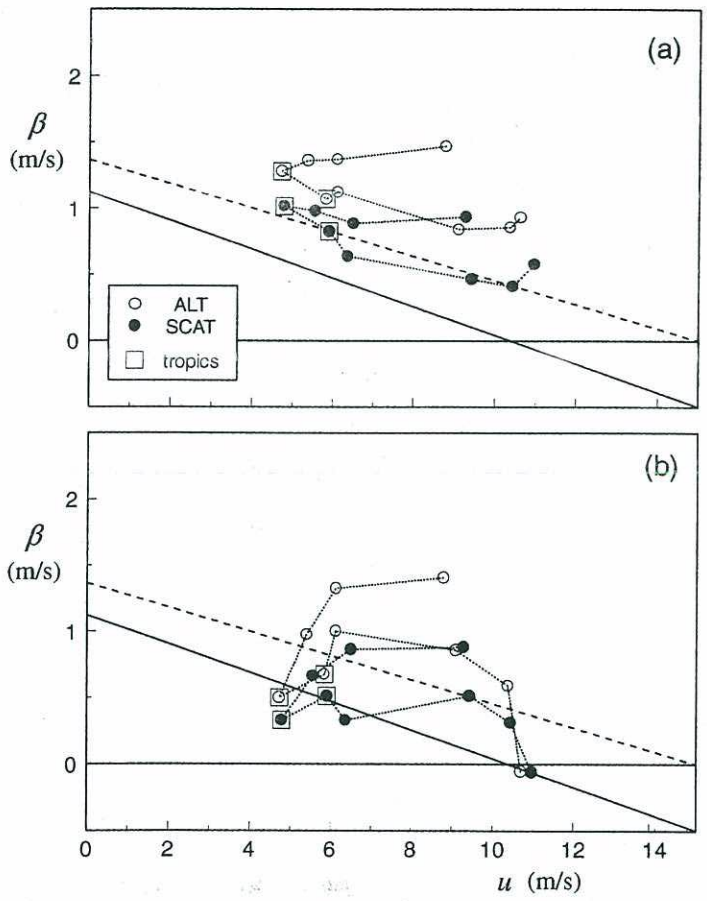

FIGURE 10 Mean biases as a function of mean wind speeds for nine consecutive latitude bands of 15° from 60°S to 75°N as obtained from ALT and SCAT data. The label 'tropics' identifies the area for 15°N to 15°S. Dotted lines connect results for consecutive bands for same instrument. Solid line: Eq. (4). Dashed lines: Eq. (5). (a) GDAS. (b) AVN.

bands are found. Mean wind speeds reduce up to the tropics, and increase again in the southern hemisphere.

The satellite data sets show consistent results with differences well within uncertainties of the bias removal (particularly if the potential effect of wave climate on altimeter observations is considered). The GDAS biases (panel a) show systematic differences between the northern and southern hemisphere, with larger biases in the southern hemisphere. These biases are furthermore similar to the biases in the southern hemisphere. These biases are furthermore similar to the biases obtained from the BA analyses (Fig. 9 left panels), suggesting that the latter biases mostly represent systematic errors. In the AVN forecast (panel b), the biases at mid latitudes remain similar, but biases in the tropics and at high northern latitudes are significantly reduced (compare panels a and b). Because such systematic errors are generally reduced, the increase of biases in the AVN according to the BA analysis (Fig. 9, compare right panels to left panels), is likely due to random model errors instead.

6. DISCUSSION

In the present study, the quality of the GDAS and AVN near-surface wind field is assessed using buoy and satellite observations as part of a systematic validation study of the new NCEP wave prediction system.

The most reliable validation results are obtained from the buoy data, although such a validation is expected to be somewhat tainted for the GDAS winds, because this data has been used in the GDAS analysis. However, the buoy data represent only a small fraction of all data, and are therefore expected to have a limited impact in GDAS. The BA analysis in Figure 2 shows that the GDAS systematically overestimates low wind speeds and underestimates high wind speeds. An underestimation of extreme wind speeds is also observed in the wind speed distributions (Tab. II). This suggests that the GDAS biases are systematic, and can be corrected statistically. Considering the results presented in Figure 2a, a linear error correction appears sufficient. Estimating the bias correction from the regression line, the bias-corrected wind speed based on buoy data ($u_{\mathrm{cor},b}$) becomes

$$u_{\mathrm{cor},b} = -1.26\,\mathrm{ms}^{-1} + 1.12u. \tag{4}$$

This error correction improves the extreme wind speed distribution of GDAS without overestimating the extreme events (Tab. II).

Compared to the buoy data, the AVN winds show significantly larger biases than GDAS (Fig. 3). However, the low bias for high wind speeds is related to random forecast errors, as the distribution of extreme wind speeds from the buoy data and the AVN are nearly identical (Tab. II). The AVN bias can therefore not be corrected statistically. Instead, it is more realistic to retain the GDAS bias correction of Eq. (4), or even reduce this correction.

Satellite wind data are less reliable than buoy data. The limited accuracy of the bias corrections and the limited capability of algorithms to retrieve extreme wind speeds reduce the accuracy of the wind speed distributions, and hence make it difficult to separate random and systematic errors. Systematic GDAS and AVN errors can nevertheless be estimated from the mean biases of Figures 8 and 10 (see previous section). The satellite derived wind speed biases are generally larger than the biases estimated from buoy observations, and indicate bias changes in the AVN winds in regions not covered by buoys. Consequently, the buoy data cannot be considered representative for a global validation.

Of the satellite data the SCAT data is most reliable and globally valid as is discussed in conjunction with Figure 7. Furthermore, NCEP's forecast responsibilities make a bias reduction in the northern hemisphere most important. Considering this, the following subjective bias correction based on global satellite data is suggested:

$$u_{\mathrm{cor},s} = -1.50\,\mathrm{ms}^{-1} + 1.10u. \tag{5}$$

This correction corresponds to a bias as depicted by the dashed line in Figure 10. This bias correction is somewhat larger than the bias correction (4) (compare solid and dashed lines in Fig. 10).

The satellite based bias correction (5) might be considered somewhat suspect for several reasons; it is based on a limited range of wind speeds (see Fig. 10) and satellite data might still incorporate significant regional biases (as discussed above). The first problem is unavoidable, as long as extreme wind speeds from satellites cannot be trusted. Without a better global coverage of ground truth data, the second point can only be addressed qualitatively by considering potential deficiencies of algorithms. For the ALT and SCAT data, these are mainly their potential dependency on wave maturity. For the SCAT data, this dependency appears negligible (Fig. 7b). Thus, the SCAT data are expected to have a consistent global validity, lending credibility to Eq. (5).

Considering the above, Eq. (5) appears a reasonable bias correction for the deep ocean. However, if this bias correction is used, validation results at the conventional buoy locations might deteriorate, erroneously suggesting a deterioration of the quality of the wind field. To avoid this, a linear combination of the bias corrections (4) and (5) can be used

$$u_{\mathrm{cor}} = \mathcal{A} u_{\mathrm{cor},b} + (1 - \mathcal{A}) u_{\mathrm{cor},s} \,, \tag{6}$$

where $\mathcal{A} = 1$ near buoys and $\mathcal{A} = 0$ in the data-sparse deep ocean. Somewhat arbitrarily, $\mathcal{A}$ is set to 1 for points in the wind field closer than 150 km to the coast or a buoy location, and to 0 for distances of over 300 km. A simple linear interpolation is used for intermediate distances. The resulting biases of the corrected GDAS winds are presented in Figure 11. As expected, the bias correction systematically reduces GDAS biases (compare Figs. 8 and 11). The remaining biases against the SCAT data are fairly evenly distributed, with slightly positive biases in the southern hemisphere as might be expected. Note that negative biases against the ALT data are concentrated in the tropics, where the wave field is often dominated by swell penetrating from higher latitudes. This behavior is therefore likely related to contamination of ALT data by swell.

The above wind speed corrections are moderate, and are expected to have a noticeable impact within the wave forecast system. The GDAS and AVN, however, are continuously being upgraded and improved. This implies that the wind speeds have to be monitored continuously, and that the bias corrections have to be upgraded periodically. In particular it should be noted that the boundary layer treatment has been modified significantly in the fall of 1995 (Chaplan *et al.*, 1997), and that the change is expected to make the surface winds more energetic. The results presented here are therefore not necessarily representative for the present products of NCEP.

In validating wave models, altimeter data are particularly interesting as their collocated wind and wave observations potentially allow for a separation of wave model errors from wind errors. This requires, however, accurate and unbiased wind estimates. A well documented deficiency of the ALT wind data is its saturation behavior for high wind speeds (see introduction and discussion of Fig. 9)[1]. Such saturation behavior is obviously detrimental for model validation in extreme conditions, but might

[1] Figure 9 suggests that the SCAT and ALT data have similar saturation behavior. This behavior of SCAT data is not well documented.

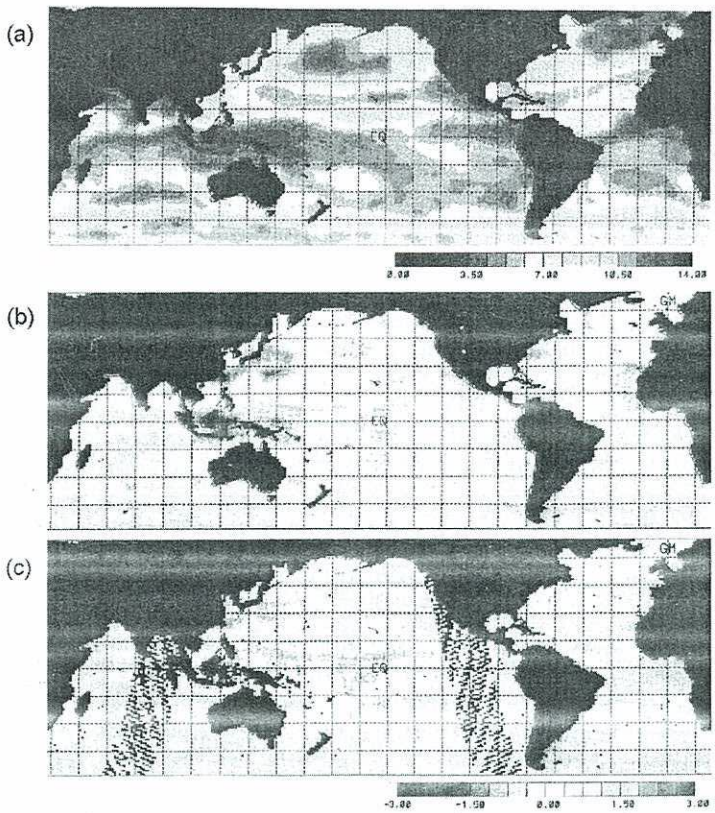

FIGURE 11 Like Figure 8 for GDAS wind fields after bias correction of Eqs. (4) through (6). (See Color Plate II).

be correctable (Young, 1993). More detrimental is the distinct dependence of the ALT wind speed on the development stage of the wave field in Figure 7a. The latter figure suggests a retrieval algorithm of the form

$$u_{\text{alt}} = Uf(\tilde{H}). \tag{7}$$

where U is the wind speed estimate for a given altimeter signal and wave condition, and where $f(\tilde{H})$ is a correction to account for the actual stage of wave development. If the nondimensional wave height $\tilde{H}$ is estimated from the buoy data, it is easy to derive an algorithm that reduces the error of altimeter winds by up to 40% (equations not reproduced here). This, however, is not a true algorithm, as it implicitly depends on the true wind speed through $\tilde{H}$.

A true algorithm can be obtained if $\tilde{H}$ is be estimated directly from the altimeter data. Such a procedure has effectively been used by Monaldo and Dobson (1989); Glazman and Greysukh (1993), and Lefevre *et al.*, (1994). These studies, however, show a small to negligible impact of including wave data in the algorithm. This suggests that the corresponding version of Eq. (7) is mathematically ill-posed, and tends to amplify random observation errors.

Alternatively, $\tilde{H}$ can be estimated independently, for instance from a wave model. This implies that an independent estimate of the wind speed is used as an integral part of the algorithm. Such an algorithm could be considered as a data assimilation scheme, where the altimeter observation is used to correct the independent 'first-guess' wind field that is used to estimate $\tilde{H}$. The final result of such a scheme by definition will be a blend of the first-guess winds and winds that are obtained from altimeter information only. The dependency of the wind speed estimates on the development stage of the wave field might therefore be reduced, but will qualitatively remain similar.

Thus, altimeter wind speeds are bound to be contaminated by the development stage of the wave field. Consequently, it does not appear prudent to use this data in an attempt to separate input and model errors in a wave model.

7. CONCLUSIONS

The quality of NCEP's analyzed (GDAS) and forecasted (AVN) surface wind fields is assessed using buoy and satellite data as a first part of the validation of a new wave forecast system. Deep-ocean wind fields are shown to incorporate moderate systematic errors, for which statistical corrections are suggested. Conventional buoy data cannot be considered representative for a global validation of marine wind fields, because the magnitude of biases based on buoy data differs systematically from global satellite derived biases, and because the buoy data do not cover several regions where the satellite data suggest regional bias changes during the forecast.

The altimeter wind data (ALT) as used here are also of interest for the direct validation of wave models, as they are always collocated with wave observations. As illustrated in other studies, the ALT data are not reliable for high wind speeds, where the conventional algorithm shows saturation behavior. Furthermore, these data are seriously contaminated by the development stage of the wave field. These wind data should therefore probably not be used to validate wave models.

Acknowledgements

The author likes to thank B. Balasubramaniyan and V. Gerald for their help in archiving and managing the data, and L. Burroughs, D. B. Rao, V. Krasnopolsk, J. Sienkiewicz and the two anonymous referees for comments on early drafts of this paper.

References

Brown, G. S. (1979) Estimation of surface wind speeds using satellite-borne radar measurements at normal incidence. *J. Geophys. Res.*, **84**, 3974–3978.

Brown, R. A. (1983) On a satellite scatterometer as an anemometer. *J. Geophys. Res.*, **88**, 1663–1673.

Caplan, P. J., Derber, W., Gemmill, W., Hong, S.-Y., Pan, H.-L. and Parish, D. (1997) Changes to the 1995 NCEP operational medium-range forecast model analysis/forecast system. *Wea. Forecasting*, **12**, 581–594.

Derber, J. C., Parish, D. F. and Lord, S. J. (1991) The new global operational analysis system at the National Meteorological Center. *Wea. Forecasting*, **6**, 538–547.

Draper, N. R. and Smith, H. (1981) *Applied regression analysis*, Wiley, pp. 709

Gilhausen, D. B. (1987) A field evaluation of NDBC moored buoy winds. *J. Atmos: Oceanic Techn.*, **4**, 94–104.

Glazman, R. E. and Greysukh, A. (1993) Satellite altimeter measurements of surface wind. *J. Geophys. Res.*, **98**, 2475–2483.

Glazman, R. E. and Pilorz, S. H. (1990) Effects of sea maturity on satellite altimeter measurements. *J. Geophys. Res.*, **95**, 2857–2870.

Kanamitsu, M. (1989) Description of the NMC global data assimilation and forecast system. *Wea. Forecasting*, **4**, 335–243.

Kanamitsu, M., Alpert, J. C., Campana, K. A., Caplan, M. P., Deaven, D. G., Iredell, M., Katz, B., Pan, H.-L., Sela, J. and White, G. H. (1991) Recent changes implemented into the global forecast system at NMC. *Wea. Forecasting*, **6**, 425–435.

Lefevre, J. M., Barckicke, J. and Ménard, Y. (1994) A significant wave height dependent function for TOPEX/POSEIDON wind speed retrieval. *J. Geophys. Res.*, **99**, 25,035–25,049.

Lindley, D. V. (1947) Regression lines and the linear functional relation. *J. Roy. Statist. Soc., Ser. B*, **9**, 218–244.

Lorenc, A. C. (1986) Analysis methods for numerical weather prediction. *Quart. J. R. Met. Soc.*, **112**, 1177–1194.

Monaldo, F. (1988) Expected differences between buoy and radar altimeter estimates of wind speed and significant wave height and their implications on buoy-altimeter comparisons. *J. Geophys. Res.*, **93**, 2285–2302.

Monaldo, F. and Dobson, E. (1989) On using significant wave height and radar cross section to improve radar altimeter measurements of wind speed. *J. Geophys. Res.*, **94**, 12,699–12,701.

Offiler, D. (1994) The calibration of ERS-1 satellite scatterometer winds. *J. Atmosph. Ocean. Tech.*, **11**, 1002–1017.

Parish, D. and Derber, J. (1992) The National Meteorological Center's spectral statistical interpolation analysis system. *Mon. Wea. Rev.*, **120**, 1747–1763.

Pierson, W. J. (1983) The measurement of synoptic scale wind over the ocean. *J. Geophys. Res.*, **88**, 1683–1708.

Ricker, W. E. (1973) Linear regression in fishery research. *J. Fishery Research Board of Canada*, **30**, 409–434.

Tolman, H. L. (1991) A third-generation model for wind waves on slowly varying, unsteady and inhomogeneous depths and currents. *J. Phys. Oceanogr.*, **21**, 782–797.

Tolman, H. L. (1998) Effects of observation errors in linear regression and bin-average analyses. *Quart. J. Roy. Meteor. Soc.*, **124**, 897–917.
Witter, D. L. and Chelton, D. B. (1991) A geosat altimeter wind speed algorithm and a method for altimeter wind speed algorithm development. *J. Geophys. Res.*, **96**, 8853–8860.
Young, I. R. (1993) An estimate of the Geosat altimeter wind speed algorithm at high wind speeds. *J. Geophys. Res.*, **98**, 20,275–20,285.

APPENDIX: OBSERVATION ERRORS

Observation errors for marine wind speeds have been investigated by, for instance, Brown (1983); Pierson (1983); Gilhausen (1987) and Monaldo (1988). Several types of errors can be distinguished, for instance, instrument errors, round-off errors due to data transmission and archiving, and mismatch errors in collocation and in representative scales (known as the representativeness error in data assimilation; Lorenc, 1986). An honest model validation considers observations which are representative for the parameters predicted by the model. Mismatch errors thus should be considered as a part of the observation error.

For the present buoy observations, the minimum observation error ($\sigma_{b,\min}$) consist of a 3% instrument error, and a round-off error ($\sigma_r = 0.15\,\mathrm{ms}^{-1}$) due to the archiving (Tolman, 1998)

$$\sigma_{b,\min}(u_o) = \sqrt{(0.03\,u_o)^2 + \sigma_r^2}. \tag{A1}$$

Representativeness errors arise due to collocation and scale mismatch errors in space or time. Estimates for such errors can be obtained from Pierson (1983); Gilhausen (1987) and Monaldo (1988) (henceforth denoted as P83, G87, and M88, respectively). A tally of error estimates for buoy observations is presented in Table AI, and a brief explanation of the estimates is given below.

The buoy wind speeds represent point observations averaged over 8.5 min. The NCEP wind fields represent synoptic wind fields with inherent scales of approximately 100 km and 1 hour. The ALT and SCAT observations are nearly instantaneous, with a footprint of $6.5 \times 65\,\mathrm{km}^2$, and a diameter of 50 km, respectively. As GDAS and AVN winds at buoy locations are interpolated, collocation errors effectively become a part of the scale error. Collocation errors of buoy and satellite data can be estimated directly from spatial and temporal separation data in G87 and M88, considering that the variability has to be divided over both locations. For the GDAS and AVN wind fields, errors of time scale differences are

TABLE AI Estimates of mean buoy observation errors in percent for GDAS, AVN, ALT, and SCAT wind speeds. The total relative error γ_0 is based on a global mean wind speed of 8 m/s, and represents a low, best and high estimate, respectively. Instrument and round-off error 3.5%

		Collocation		*Scales*		*Total relative error*		
		space	*time*	*space*	*time*	γ_0 (%)		
GDAS,	P83				6–9	10.1	13.0	15.4
AVN	G87	0		12	5			
	M88			8–10	8			
ALT	P83				3–5	11.2	13.5	15.0
	G87	12		6	3			
	M88	9–11	3	4–5	4			
SCAT	P83				2–3	7.7	8.8	9.9
	G87	6		4	2			
	M88	5–6	3	2–3	3			

presented in all three papers, and errors for spatial scale differences can be estimated from spatial separation data in G87 and M88. According to M88, the representative scales of the SCAT winds are fairly similar to those of the buoy, whereas the ALT scales are smaller. Somewhat arbitrarily, the scale errors have been taken as 1/2 or 1/3 of the corresponding error of the buoy observations relative to the GDAS and AVN fields.

Table AI presents expected average observations errors $\overline{\sigma}_{b,o}$ (or mean error fractions γ_0) for the buoy observations, but not the error distribution over wind speeds required for the BA analyses. Scale errors generally increase with wind speeds; approximately linear for time averaging (P83), and somewhat stronger for space averaging (M88). Unfortunately, collocation errors have not been assessed as a function of wind speed. It appears natural to assume that the overall error increases approximately linearly for higher wind speeds, and is finite for small wind speeds. This suggests a shape of the observation error similar to Eq. (A1).

$$\sigma_{b,o}(u_o) = \sqrt{(\alpha\overline{\sigma}_{b,o})^2 + (\gamma u_o)^2}, \tag{A2}$$

where $0 < \alpha < 1$. Furtheremore requiring that γ_0 as presented in Table AI is reproduced for the mean wind speed $\overline{u_o}$, the asymptotic error fraction γ becomes

$$\gamma = \gamma_0\sqrt{1 - \alpha^2}. \tag{A3}$$

Somewhat arbitrarily, $\alpha = 0.7$ will assumed, corresponding to $\gamma/\gamma_0 = 0.71$. To assess uncertainties in this assumption, a range of $0.6 < \alpha < 0.8$ ($0.8 > \gamma/\gamma_0 > 0.6$) will be used in the calculations.

The BA analyses in Section 5 require an estimate of the satellite observation errors relative to the GDAS and AVN winds. The relatively large random instrument errors (Figs. 5b and 6b) imply that these observation errors are likely dominated by instrument errors. Furthermore considering that biases cannot be removed accurately, simple estimates for the observation error as gathered in Table IV have been adopted.